Environmental Pollution 363 (2024) 125069

Contents lists available at ScienceDirect

Environmental Pollution

journal homepage: www.elsevier.com/locate/envpol

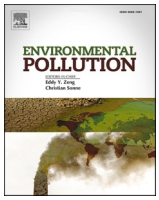

Electrolysis of HTL-AP for nutrient recovery by converting cyclic nitrogen to nitrate-N fertilizer☆

Barbara Camila Bogarin Cantero, Yuanhui Zhang, Paul C. Davidson *

Department of Agricultural and Biological Engineering, University of Illinois at Urbana Champaign, Urbana, IL, 61801, USA

ARTICLE INFO

Keywords:
Wastewater
Storage stability
Nutrient recovery
Nitrogen cyclic compounds
HTL-AP
Nitrate

ABSTRACT

Valorization of hydrothermal liquefaction aqueous phase (HTL-AP) can be achieved through its use as a nutrient source for lettuce production in hydroponic systems after being treated to reduce the nutrient imbalance. Removing nitrogen cyclic compounds in HTL-AP may impact the availability of some nutrients, such as nitrate-N, that are necessary for plant growth. Previous studies indicate that electrolysis enables nitrate-N accumulation in algal-HTL-AP. In this study, HTL-AP derived from food waste was electrolyzed to convert available nitrogenous compounds into nitrogen forms that are preferred by plants such as nitrate-N. Biochemical properties were assessed for the HTL-AP samples before and after two years of storage. Results from this study show that it is viable to convert heterocyclic amines in HTL-AP into inorganic nitrogen forms such as nitrite-N, nitrate-N, ammonia-N, and fatty acids. Specifically, this study showed that accumulation of 609 mg/L of nitrate-N in the HTL-AP with an initial concentration of 25 mg/L was achieved at the lowest current density. Additionally, electrolysis treatment removed 48%–61% of COD from the HTL-AP at different current densities. Furthermore, water quality characterization before and after storage for two years showed decreased organic matter in the HTL-AP, leading to reduced inorganic nitrogen recovery. Overall, this study indicates that electrolysis can increase the concentration of inorganic nitrogen in the HTL-AP both before and after long-term storage.

1. Introduction

Hydrothermal Liquefaction (HTL) has the potential to process and recycle wet food waste to produce renewable energy (Aierzhati et al., 2019; Biller et al., 2012). While HTL shows promise for converting wet biomass into biocrude oil, current technologies for valorizing the aqueous phase product (HTL-AP) of the reaction are limited, due to the large volumes of this wastewater and lack of proper treatment methods for reutilization (Watson et al., 2020). The products of the reaction and composition of HTL-AP depend on the feedstock composition (He et al., 2020; SundarRajan et al., 2021a; Halleraker & Barth, 2020; Jiang et al., 2020) and reaction conditions (Swetha et al., 2021a; Wu et al., 2020; León et al., 2019).

Current approaches for valorization of HTL-AP utilize recirculation in the HTL reaction (Z. Zhu et al., 2015). However, due to the composition of the HTL-AP, it decreases the quality of the biocrude oil (Kohansal et al., 2021; Pedersen et al., 2016; Harisankar et al., 2021). Another method of valorizing the HTL-AP is by recycling nutrients through algae production (Godwin et al., 2017) or third generation bioenergy feedstock (Biller et al., 2012). The utilization of nitrogen and phosphorus for algal growth (Garcia Alba et al., 2013) and other nutrients that contribute to the cultivation of microalgae and fungi (J. Chen et al., 2022) has also been reported. Moreover, HTL-AP has been utilized for lettuce (*Lactuca sativa*) cultivation as a nutrient solution, but growth inhibitors and nutrient imbalance negatively influenced plant growth (Jesse and Davidson, 2019; Jesse et al., 2019).

HTL-AP contains nitrogenous compounds and organic acids that are frequently produced during the liquefaction of proteins and carbohydrates (SundarRajan et al., 2021a). These compounds, which include phenolics, cyclic ketones, pyrroles, pyrazines, and amines in HTL-AP have been suggested to be algae growth inhibitors due to effects in chlorophyl formation (McGinn et al., 2019). Micro and macronutrients that are critical for algal development and support photosynthesis are lost during the HTL process (SundarRajan et al., 2021b). In addition, organic compounds in HTL-AP may inhibit algal growth (Swetha et al., 2021b; Y. Zhu et al., 2019). Therefore, treatment of HTL-AP is needed to reduce growth inhibitors such as phenols, ammonia-N, and organic nitrogen compounds (Leng et al., 2020). It should be noted, however, that

☆ This paper has been recommended for acceptance by Dr. Meththika Vithanage.

* Corresponding author.
E-mail address: pdavidso@illinois.edu (P.C. Davidson).

https://doi.org/10.1016/j.envpol.2024.125069
Received 9 July 2024; Received in revised form 24 September 2024; Accepted 1 October 2024
Available online 5 October 2024

the recycling of HTL-AP represents an economic investment due to energy usage (Godwin et al., 2017). While treatments such as anaerobic digestion have been used to treat HTL-AP to absorb nutrients and toxins, HTL-AP contains aromatics, nitrogen heterocyclic compounds, and furanics that are known to inhibit biological treatment (Yang et al., 2020; Egerland Bueno et al., 2020; Z. Wang et al., 2021; Wang et al., 2021). Other treatments, such as ozone, can remove some of the organic matter, which usually acts as an inhibitor of microorganisms, from the HTL-AP (Si et al., 2019). Sand filtration has been used to reduce the concentration of growth inhibitors in HTL-AP, however, it also reduced the concentration of plant-available nitrogen (Jesse et al., 2019). Other methods, such as activated carbon, can reduce the toxicity of the HTL-AP (H. Wang et al., 2021; P. H. Chen et al., 2020), but may also decrease the concentration of nitrogen forms that could be taken up by plants (Jesse and Davidson, 2019). Previous studies have attempted to valorize the HTL-AP with fungal treatment (Leme et al., 2024a; Lopez et al., 2024) and lettuce growth (Reynolds et al., 2024). However, they utilized diluted HTL-AP for their studies. Recently, a treatment with electrochemical oxidation reported a high removal of chemical oxygen demand (COD), which is an indicator for the concentration of oxidizable matter of the effluent (Hu & Grasso, 2005), while increasing the production of nitrate-N and ammonia-N as final inorganic compounds without dilution (Ciarlini et al., 2020a). This treatment represents an opportunity to transform recalcitrant molecules that are not removed by biological treatment in the water (Anglada et al., 2009). Additionally, because a large volume of wastewater is produced during each HTL run, storage conditions could become a limiting factor over time. Therefore, the objectives of this work are to; a) evaluate the effectiveness of electrolysis as a treatment for food waste derived HTL-AP to convert nitrogen-containing aromatics into plant-available nutrients using conductive anodes at different current densities for nitrate-N accumulation in HTL-AP, b) assess the impact of storage at room temperature on the nutrient profile of HTL-AP, and c) evaluate differences in electrolysis treatment performance under different initial water quality characteristics of the HTL-AP.

2. Materials and methods

2.1. HTL-AP characterization

Hydrothermal liquefaction aqueous phase (HTL-AP) was obtained from a hydrothermal liquefaction (HTL) pilot reactor (Aierzhati et al., 2021; Summers et al., 2023) at 280 °C ± 20, 1800 psi, and with a retention time of 30 min, using food waste as the feedstock. The first set (pre-storage) of HTL-AP was analyzed for ammonia-N (Hach Method 10031), COD (Hach Method 8000), nitrate-N-nitrogen (Hach Method 10020), nitrite-N-nitrogen (Hach Method 8153), and pH (Cole Parmer PC 100, IL, USA) after electrolysis. The second set (post-storage) was analyzed after two years of storage for the same parameters, plus pH using a HALO Wireless pH Meter with Microbulb (Hannah Instruments, RI, USA). Hach Method 10019 was used here because the levels of nitrite-N in the post-storage HTL-AP were not detected with the high range method listed above.

To assess changes in the HTL-AP due to treatment, the water quality measurements described above were conducted before and after each treatment. In addition, GC-MS analysis of the pre-storage HTL-AP samples, before and after treatment, were done at the Carver Metabolomics Core (University of Illinois Roy J. Carver Biotechnology Center, IL, USA). To obtain the removal and accumulation of the compounds after electrolysis of HTL-AP, the difference between the initial peak area of the compounds, pre-treatment, and the final peak area values of the compounds, post-treatment, was taken, divided into the initial value, and multiplied by 100 to express the result as a percentage.

2.2. Electrolysis of HTL-AP derived from food mixture

An electrochemical cell with a two-electrode system containing HTL-AP was degassed with argon gas for 20 s. The two electrodes (anode and cathode) were placed inside the cell with an inner electrode gap of 2 cm. The anode material used was Boron Doped Diamond (IKA, NC, USA) and the cathode material was stainless steel (IKA, NC, USA) with dimensions of 52.5 mm by 8 mm by 2 mm. The first set of experiments (pre-storage) were performed in duplicate, and the second set of experiments (post-storage) was performed in triplicate. The system was supplied with constant current from a DC power supply Siglent SPD3303C (TEquipment, NJ, USA) and Instek GPD-4303S DC Power Supplies 4 Channels (TEquipment, NJ, USA). The electrical conditions were achieved using the Easy Power Software and voltage, current, and time were collected utilizing a Python program. The experiments were performed in batch recirculation utilizing a cell containing a total of 60 mL of HTL-AP that was continuously recirculated between a small electrochemical cell with 20 mL of HTL-AP and the 40 mL reservoir. The 20 mL volume was selected to ensure that the electrodes were in continuous contact with at least 3 mL of the sample (Fig. 1). The pre-storage experiments utilized a custom pump fabricated in-house and for the post-storage experiments, the pump was upgraded to easy pump VI-Shenchen Baoding (Darwin Microfluids, Paris, France) to increase the reliability and durability of operation of continuous pumping over long periods of time.

To ensure the electrodes were in contact with the wastewater, peristaltic pumps were used to generate a flow rate of 20 mL/min to recirculate the HTL-AP from the electrochemical cell to the reservoir. After each experiment, the electrodes were cleaned with a 0.1 M H_2SO_4 solution in an ultrasound bath for 10 min and then rinsed with deionized water. To evaluate the optimal conditions for organic nitrogen conversion into inorganic nitrogen forms, three current densities were tested: 10 mA/cm^2 (low), 30 mA/cm^2 (medium), and 50 mA/cm^2 (high). The durations of the corresponding experiments were 119 h, 40 h, and 24 h, respectively. These durations were chosen to normalize the experiments

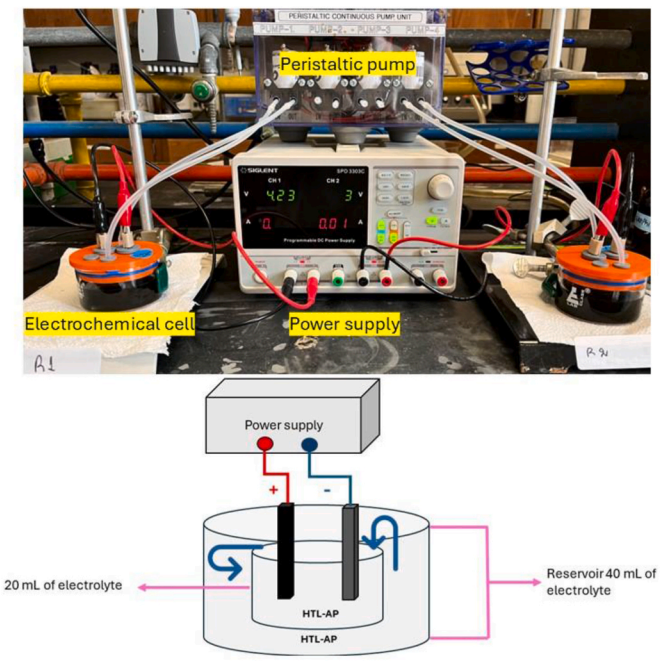

Fig. 1. Experimental set up. Top: Two electrochemical cells with the batch recirculation system and the power supply for pre-storage HTL-AP experiments; Bottom: Diagram of the experimental setup, used for both the pre- and post-storage experiments, where the electrochemical cell has a smaller glass container for 20 mL of the electrolyte and a larger glass container with 40 mL of the electrolyte.

and obtain a total charge consumption of 10 A h for all three current densities.

Samples consisting of 400 μL of HTL-AP were taken from the reactor every 2 A h and diluted to perform the water quality analyses. The electrolysis process was conducted at room temperature. No modifications (dilutions, pH adjustment, temperature increase, or addition of salts) to the raw HTL-AP were applied for these experiments, as they may alter the kinetics of the reaction.

3. Results and discussion

3.1. HTL-AP food mixture characterization

The observed chemical oxygen demand (COD) prior to being stored was 26,800 mg/L, which is within the range of frequently reported values of 20,000–120,000 mg/L COD (Leng et al., 2018). Low levels of nitrate-N (NO_3-), nitrite-N (NO_2-), and ammonia-N (NH_3-N) were also observed (Table 1).

Generally, the pH of the HTL-AP depends on the biomass composition; in this case the feedstock used for the HTL reaction was low in protein. Therefore, it did not contain a high concentration of ammonia-N from deamination of protein through hydrolysis. The pH was within the range of 3–10; as reported in the literature, it depends on the biomass composition in the HTL (Leng et al., 2018). The HTL-AP generated from food waste has been reported to be more acidic due to the presence of organic acids as degradation products of carbohydrates in the feedstock during the HTL process (Maddi et al., 2017).

Biomass-derived oils and fractions have shown to be chemically and physically unstable under different storage temperatures and times (Liu et al., 2021). Water characterization from before and after storage for two years (Table 1) follows this previous finding by showing three major changes in the water quality characteristics of the HTL-AP after storage. First, the COD decreased by approximately 76%. Second, in terms of nitrogen availability, the ammonia-N and nitrate-N concentrations increased by 1% in the HTL-AP, while the nitrite-N concentration decreased. Third, the pH in the wastewater increased. Although the aqueous phase has shown to be more stable than the bio-oil after storage at different temperatures and times, the aqueous phase has still been reported to decrease in concentration of all chemical groups with aging and different storage temperatures (Ren & Ye, 2018), which aligns with the chemical changes in HTL-AP after storage in this study, as shown in Table 1.

The GC-MS analysis of food waste derived HTL-AP, pre-storage, showed the presence of amines, carboxylic acids, and alcohol, which are reduced species that perform oxidation reactions, and the ketones that perform reduction reactions because they are oxidized species (Forster, 2019) (Table 2). As highlighted in Table 2, the aim of electrolysis in this study is the conversion of heterocyclic amines into nitrate and ammonia.

3.2. Effect of current on carbon reactions

Water quality characterization results indicate that utilizing electrolysis led to degradation of COD in the HTL-AP for all current densities and initial concentrations of organic matter tested in this study. For the first set of experiments (pre-storage) when the initial COD concentration was 26,800 ± 1476, 58%, 61%, and 49% of the oxidizable organic matter was removed at 10 mA/cm^2, 30 mA/cm^2, and 50 mA/cm^2, respectively, after the treatment (Fig. 2a). Comparatively, for the second set of experiments (post-storage) with a relatively low initial COD concentration of 6,340 ± 639, 62%, 76%, and 69% of the organic matter was removed at 10 mA/cm^2, 30 mA/cm^2, and 50 mA/cm^2 after electrolysis (Fig. 2b).

Fig. 2a shows that at a higher initial concentration of oxidizable organic matter, 30 mA/cm^2 and 10 mA/cm^2 achieved a higher removal of COD by the end of the treatment. As indicated in the figure, during the first hours of treatment, the higher current density slightly improved the removal of COD in the HTL-AP, resulting in 30% higher removal of organic matter after applying 50 mA/cm^2 compared to 30 mA/cm^2. Carbon mineralization increased until 2 A h, achieving a concentration of 7,643 mg/L of COD, and later, only 20% of COD was removed at 8 A h. The exponential removal of COD and the sudden and continuous decrease in the removal percentage after 2 A h indicates the carbon removal at 50 mA/cm^2 is governed by mass transfer, or the availability and diffusion of the organic compounds in the HTL-AP (Ciríaco et al., 2009; Díaz et al., 2011). The decrease in COD removal could have also been due to the presence of some refractory organic compounds that cannot be further oxidized, or possibly due to reduction reactions and competitive reactions (Panizza et al., 2001a). As suggested by a study of disinfection with electrochemical oxidation, a higher current density leads to the production of hydroxyl radicals that induce oxidation, but as the treatment advances, there is a decrease in efficiency of oxidation of organic matter, which could have been caused by undesirable reactions in the HTL-AP (Hughes et al., 2023).

Since COD represents the organic oxidizable materials in the water (Zhao et al., 2004), the 30 mA/cm^2 current density had a higher COD removal, or oxidation efficiency, compared to the other tested current densities. Since the removal was steady and consistent during the treatment period, this might be explained by Faraday's law, as the current increases the amount of oxidizable and reducible species on the anode surface (Sundén, 2019; Fil et al., 2014). However, there is a tradeoff between time and removal of COD. As seen with the 10 mA/cm^2

Table 1
Characterization of HTL-AP from a mixture of food waste before, and after, a storage time of two years, but without any treatment.

Analysis	pre-storage HTL-AP (n = 2)		post-storage HTL-AP (n = 3)	
	Average (mg/L)	SD (mg/L)	Average (mg/L)	SD (mg/L)
COD	26,800.0	1470.0	6340.0	638.8
NH_3-N	350.0	52.7	45.6	2.2
NO_3-N	25.0	5.3	37.5	0.4
NO_2-N	100.0	34.6	0.2	0.05
pH	4.5	0.01	5.2	0.2

*n: number of replicates *SD: standard deviation.

Table 2
Gas Chromatography and Mass Spectroscopy analysis of HTL-AP food mixture, pre-storage.

Name	Type of compound
2,5 hexadione	Ketone
2-butanone	
2-methyl- 2-cyclopenten-1-one	
3-methyl- 2-cyclopenten-1-one	
Acetone	
4-hydroxy-Benzenesulfonic acid	Sulphone
Acetaldehyde	Aldehyde
2,6-dimethyl-3-hydroxypiridine	Heterocyclic amine
3-Pyridinol	
6-methyl-3-Pyridinol	
Caprolactam	
Butyrolactone	
2-pyrrolidinone	
Guanidine	
trans-(n)-furan, tetrahydro-2,5-dimethyl-	
2,2′-oxybis-ethanol	Alcohol
2-propenoic acid	Carboxylic acid
4-chlorobutanoic acid	
acetic acid	
methyl ester acetic acid	
butyric acid	
Glycerin	
n-hexadecanoic acid	
propanoic acid	
Isosorbide	Alcohol
Benzenemethanol	Alcohol
dichloro methane	Organochlorade

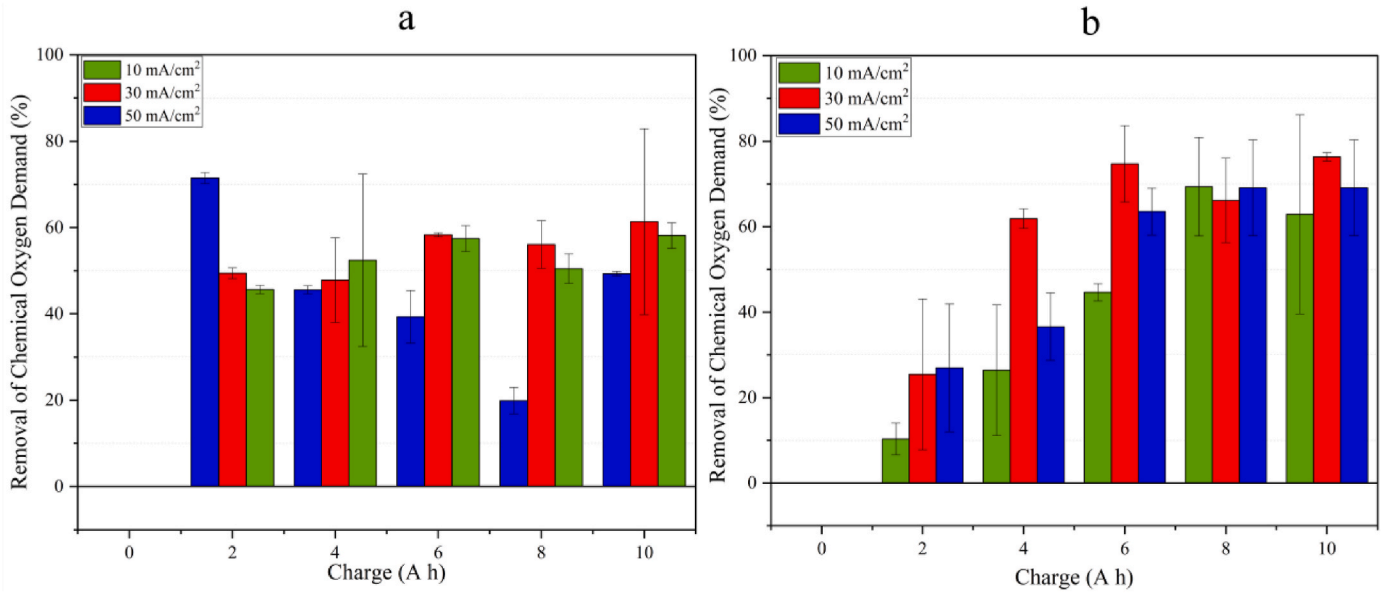

Fig. 2. Chemical oxygen demand (COD) removal from the aqueous phase of hydrothermal liquefaction food mixture pre-storage (a) and post-storage (b) as a function of charge consumed during the anodic oxidation using BDD as the anode at three different current densities. Please note at 0 Ah, no removal had occurred because no treatment was applied.

current density (Fig. 2a), there was a slow increase in removal of COD with time and it obtained 58% removal after 119 h of treatment. Comparatively, the 50 mA/cm^2 current density achieved higher removal of COD after only 4 h of treatment. The difference in removal could be due to fewer hydroxyl radicals in the surface of the electrode at a lower current density, as the increase in current density is related to a higher production of free radicals that enable oxidation reactions (Hmani et al., 2012). On the other hand, with electrolysis at 10 mA/cm^2, irrespective to the differences in initial organic load (Fig. 2b), consistent levels of COD removal were achieved with removal percentages ranging between 58% and 62% before and after storage of HTL-AP, respectively.

Similarly, Fig. 2b reveals that a lower initial concentration of COD achieved a higher removal efficiency at 30 mA/cm^2 compared to 50 mA/cm^2. These results suggest that the degradation kinetics of COD in the HTL-AP may be controlled by mass transport, as studies of organic substrates using a BDD anode have reported similar mineralization results at different initial concentrations of organic substrates (Hmani et al., 2009; Panizza et al., 2001b; Rodrigo et al., 2001). Overall, the degradation of COD was more prominent at higher current densities and with a lower initial organic matter concentration, which agrees with the mass transport behavior of electrolysis of the HTL-AP. Different initial water quality characteristics of the HTL-AP resulted in different removal efficiencies for COD. Therefore, while different feedstocks will likely also have different initial water quality characteristics, it is not possible to speculate that the same removal patterns will hold true for other feedstocks based solely on the results of this study.

3.3. Effect of current on inorganic nitrogen

Through electrolysis, nitrate-N accumulated in the HTL-AP at different current densities. However, the concentrations of nitrate-N varied by current density for both the first and second sets of experiments (before and after storage, respectively). For the first set of experiments (prior to storage), results show that lower current densities performed best for nitrate-N recovery in HTL-AP. A 10 mA/cm^2 current density produced 609.4 mg/L, 30 mA/cm^2 produced 156.3 mg/L, and 50 mA/cm^2 produced 34.9 mg/L of nitrate-N after 10 A h. Comparatively, after storage, a 10 mA/cm^2 produced 14.6 mg/L, 30 mA/cm^2 produced 17.4 mg/L, and 50 mA/cm^2 accumulated 8.3 mg/L of nitrate-N in the HTL-AP after 10 A h (Table 3). Compared to biological treatments (Jesse and Davidson, 2019; Leme et al., 2024b; Lopez et al., 2024), electrolysis achieved an overall higher nitrate-N recovery from the food waste derived HTL-AP without dilutions or pH adjustments. However, a higher nutrient recovery was achieved in microalgal HTL-AP after electrochemical treatment, however, it contained higher nitrogen levels and a higher pH (Ciarlini et al., 2020b). This highlights the relevance of the pH and the initial concentration of organic nitrogen compounds in the HTL-AP on the nitrification process through electrolysis. Subsequent studies should focus on the reaction mechanism, treatment optimization, as well scalability considering the conditions that will

Table 3
Summary of inorganic nitrogen concentrations after treatment for the pre-storage and post-storage experiments with electrolysis at 10 A h.

10 mA/cm^2						
	NH_3-N (mg/L)	SD (mg/L)	NO_3-N (mg/L)	SD (mg/L)	NO_2-N (mg/L)	SD (mg/L)
pre-storage HTL-AP	303.1	3.5	609.4	34.9	87.5	24.3
post-storage HTL-AP	234	74.7	14.6	2.9	BDL	BDL
30 mA/cm^2						
	NH_3-N (mg/L)	**SD (mg/L)**	**NO_3-N (mg/L)**	**SD (mg/L)**	**NO_2-N (mg/L)**	**SD (mg/L)**
pre-storage HTL-AP	342.2	3.5	156.3	69.8	31.3	8.20
post-storage HTL-AP	BDL	BDL	17.4	8.4	BDL	BDL
50 mA/cm^2						
	NH_3-N (mg/L)	**SD (mg/L)**	**NO_3-N (mg/L)**	**SD (mg/L)**	**NO_2-N (mg/L)**	**SD (mg/L)**
pre-storage HTL-AP	554	2.8	34.4	22.9	300	39.8
post-storage HTL-AP	7.8	4.5	8.3	2.9	BDL	BDL

*BDL: Below detection limit.

enhance the nutrient recovery.

The concentrations of nitrate-N, ammonia-N, and nitrite-N in the HTL-AP during treatment of HTL-AP prior to storage at the lowest current density tested in the study (10 mA/cm^2) are shown in Fig. 3. The beginning of the treatment shows production of nitrate-N and ammonia-N happening with a 1:1 ratio until the 6 A h mark. Noticeably, nitrite-N concentration is steady throughout the treatment, which may be attributed to its role as an intermediary byproduct that reacts to become ammonia-N, nitrate-N, or nitrogen gas during electrolysis (Ghazouani et al., 2015). Similarly, there were no detectable levels of nitrite-N and a continuous increase of ammonia-N and nitrate-N concentrations during electrolysis of HTL-AP, post-storage. It is also observed that the pH steadily increased as the ammonia-N concentration increased in the HTL-AP, post-storage (Table S1 in the Supplementary Material).

The production of nitrate-N with electrolysis was greatest with a higher initial inorganic nitrogen and organic matter concentration in the HTL-AP, pre-storage. However, the treatment successfully achieved double the inorganic nitrogen availability after electrolysis before and after storage of the HTL-AP (Table S1 in Supplementary Material), yielding approximately 1,000 mg/L and 248 mg/L of inorganic nitrogen, respectively. Low organic compound concentration in wastewater has previously been reported to limit complete nitrification and denitrification processes, which might be the cause of low nitrate yield after electrolysis of post-storage HTL-AP (Zöllig et al., 2017).

The lowest current density achieved a larger accumulation of inorganic nitrogen in the HTL-AP compared to the other tested currents in this study, before and after storage. Prior to storage and at 8 A h, the concentration of ammonia-N in the HTL-AP increased nearly 68%. This could be due to the deamination of cyclic organic products to ammonia-N instead of nitrate-N, as described in an oxidation study of an emergent contaminant or organic nitrogen compound (Olvera-Vargas et al., 2014). A slow rise in the nitrate-N concentration is observed at 10 A h after the decrease in the ammonia-N concentration in the HTL-AP, which could have been due to the oxidation process of ammonia-N to nitrate-N (Cabeza et al., 2007), which is enhanced by acidic conditions accompanied by the increasing COD removal (Ghazouani et al., 2017).

With the 10 mA/cm^2 current density, it was possible to achieve 609.4 mg/L of nitrate-N from a 25.0 mg/L starting concentration and 303.1 mg/L of ammonia-N from a 350.0 mg/L starting concentration. Moreover, nitrite-N decreased to 87.5 mg/L from a 100.0 mg/L starting concentration with HTL-AP, pre-storage. Since high ammonia-N content as well as acidic conditions could be toxic for the plants, a lower ratio of ammonia-N over the total nitrogen content (Savvas et al., 2006) of the HTL-AP is preferred for plant growth.

By looking at differences in mineralization of nitrogen in the electrolysis with 30 mA/cm^2 shown in Fig. 4 (Table S2 in the Supplementary Material), there was a higher production of ammonia-N than nitrate-N or nitrite-N in the HTL-AP prior to storage at this current density. However, it should be noted that ammonia-N production did begin to decrease at the 8 A h and 10 A h charges. Results showed that three distinct processes were taking place during electrolysis at 30 mA/cm^2: (1) ammonia-N was accumulated from organic nitrogen mineralization; (2) nitrate-N was reduced to nitrite-N; and (3) nitrite-N was converted to nitrate-N and ammonia-N in the HTL-AP. In a similar fashion, higher ammonia-N production was observed during the treatment of the HTL-AP, post-storage, and slightly lower nitrate-N yield, with no detectable levels of nitrite-N.

Prior to storage and at 2 A h, there was an increase in ammonia-N and nitrate-N in the HTL-AP. A higher concentration of ammonia-N suggests the mineralization of nitrogen cyclic compounds into inorganic ions (Jara et al., 2009). During the first 8 h of treatment (2 A h) of HTL-AP (pre-storage), nitrite-N concentration decreased while nitrate-N concentration increased by more than three times from 25.0 mg/L to 78.1 mg/L (Table S2 in the Supplementary Material). Additionally, ammonia-N increased 60% from 350.0 mg/L to 937.5 mg/L. A higher accumulation of ammonia-N in HTL-AP may be attributed to the nature of the electrode utilized in the experiments, since it was reported in the literature that doped diamond electrodes have high faradaic efficiency for ammonia-N production (Tenne et al., 1993). Furthermore, this type of electrode has a limitation for ammonia-N production; a saturation period which leads to the development of intermediaries such as nitrate-N and nitrite-N in the electrolyte (Tenne et al., 1993). This is observed at 4 A h when the concentration of ammonia-N, as well as nitrite-N, decreased while the nitrate-N concentration doubled. Also, at 6 A h, nitrate-N, nitrite-N, and ammonia-N proportions remain steady as a product of deamination of organic nitrogen compounds in the HTL-AP pre-storage. However, the highest concentration of all inorganic nitrogen forms was achieved at 30 mA/cm^2 in the HTL-AP prior storage

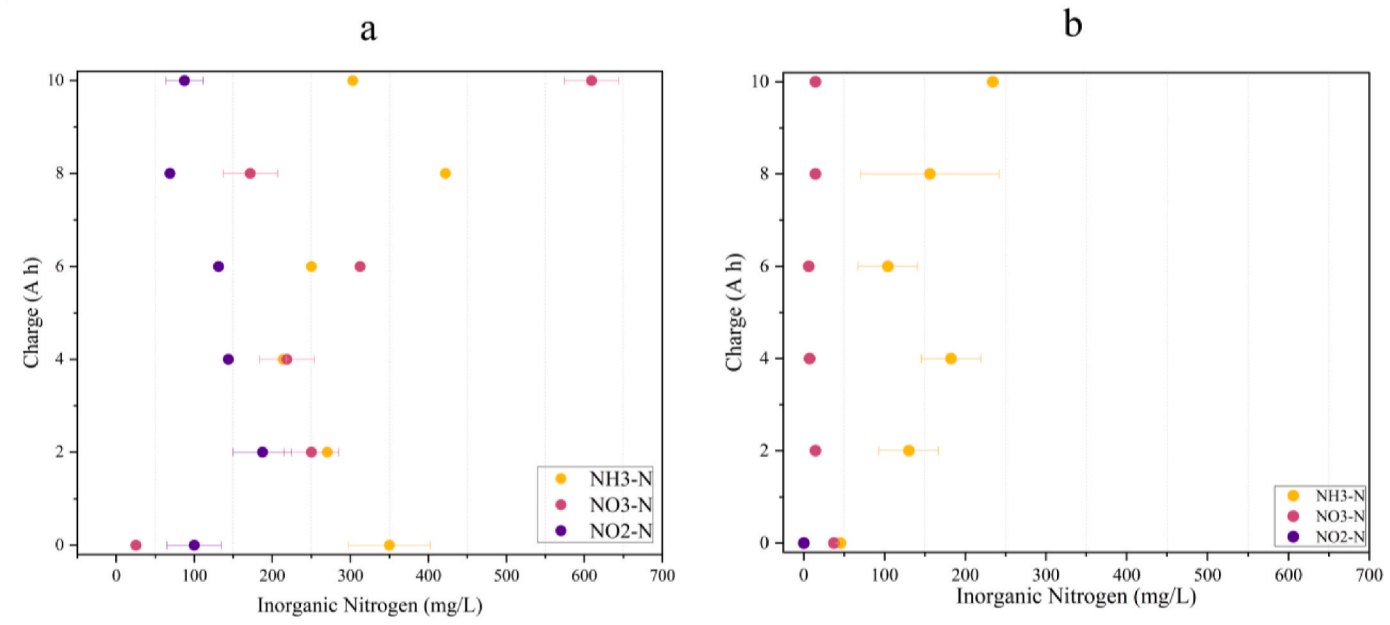

Fig. 3. Concentrations of inorganic nitrogen profile in the aqueous phase of hydrothermal liquefaction food mixture pre-storage (a) and post-storage (b) during electrolysis using BDD anode at 10 mA/cm^2.

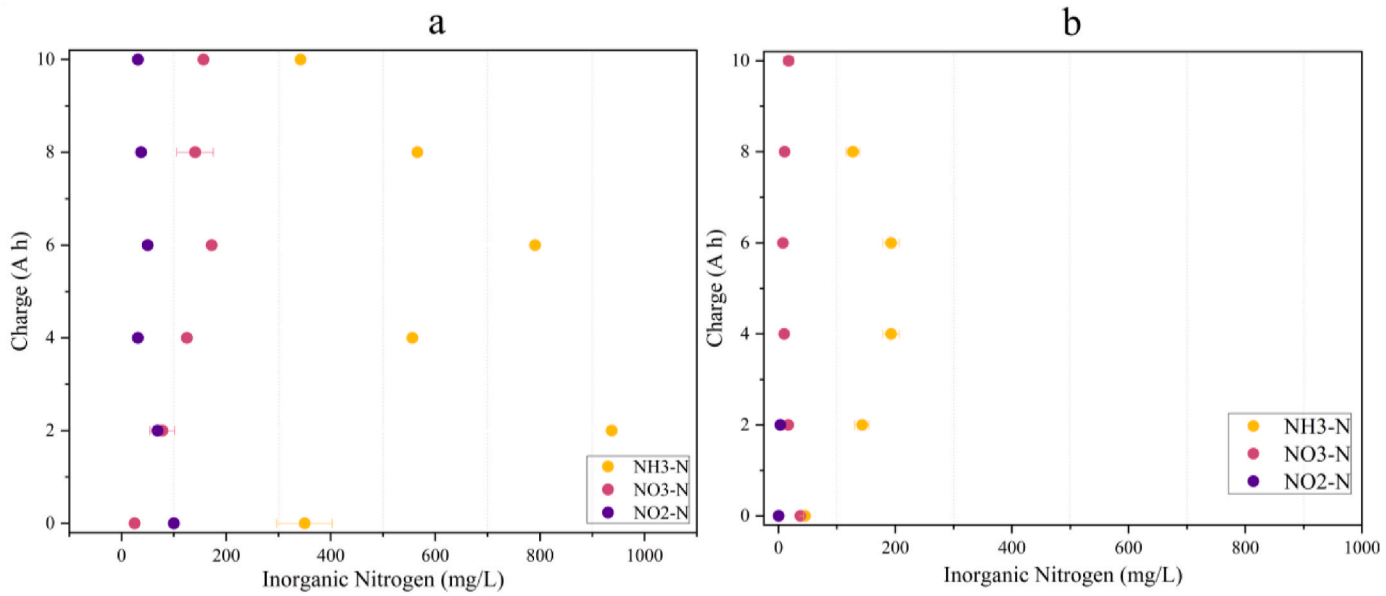

Fig. 4. Concentrations of inorganic nitrogen profile in the aqueous phase of hydrothermal liquefaction food mixture pre-storage (a) and post-storage (b) during electrolysis using BDD anode at 30 mA/cm^2.

(Fig. 4). In addition, in the HTL-AP pre-storage, at 8 A h, the nitrate-N concentration increased by 2% in the HTL-AP in the relative distribution of inorganic nitrogen forms, but as seen in Fig. 4 (Table S2 in the Supplementary Material), all inorganic nitrogen forms decreased in concentration compared to 6 A h, which could have been caused by its conversion to nitrogen gas, as a lower concentration of nitrogen species remained in the HTL-AP after the treatment. A similar behavior (decrease of ammonia-N) was reported in previous studies (dos Santos et al., 2021). However, it is difficult to comment on the ammonia-N conversion to its volatile intermediaries without an analysis of the gas production during electrolysis, which was beyond the scope of this study.

By the end of the treatment of the pre-storage HTL-AP, ammonia-N accounted for 65% of all the inorganic nitrogen forms, while nitrate-N accounted for 29%. Although 156.3 mg/L of nitrate-N was accumulated in the pre-storage HTL-AP at 30 mA/cm^2, this operational condition primarily seemed to enhance the conversion of organic nitrogen compounds into ammonia-N.

On the other hand, after storage with lower organic matter concentrations and initial inorganic nitrogen, only 16.7 mg/L of nitrate-N was recovered, and no detectable levels of ammonia-N nor nitrite-N were observed in the post-storage HTL-AP by the end of the treatment at this current density. Despite the low nitrate-N recovery in the post-storage HTL-AP, with electrolysis, it was possible to yield the highest levels of inorganic nitrogen at 2 A h, 4 A h, and 6 A h, where 163 mg/L, 200 mg/L, 200 mg/L of overall inorganic nitrogen concentration were detected, respectively.

Electrolysis at 50 mA/cm^2 seemed to have enabled the removal of

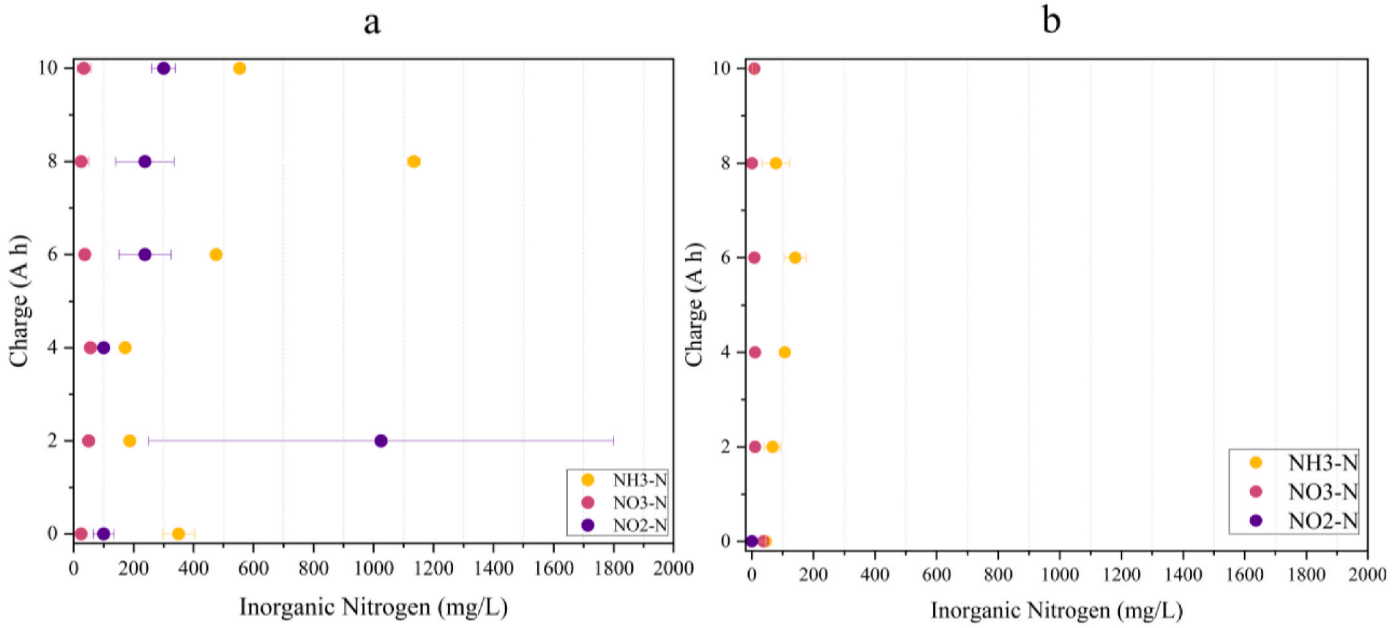

Fig. 5. Concentrations of inorganic nitrogen profile in the aqueous phase of hydrothermal liquefaction food mixture pre-storage (a) and post-storage (b) during electrolysis using BDD anode at 50 mA/cm^2.

inorganic nitrogen in the HTL-AP, both pre- and post-storage (Fig. 5). Compared to the lower current densities tested in this study, low accumulation of nitrate-N was achieved after treating the HTL-AP, pre-storage, with 50 mA/cm^2 of electrolysis, obtaining only 34.4 mg/L of nitrate-N. In the same way, in the post-storage treated HTL-AP, only 8.3 mg/L of nitrate-N was detected at 10 A h (Table S3 in the Supplementary Material).

During the first hours of treatment of pre-storage HTL-AP, there was a higher nitrite-N concentration than ammonia-N and nitrate-N. Later, the nitrite-N concentration decreased while there was a continuous increase in ammonia-N concentration in the pre-storage HTL-AP until 8 A h, when 50 mA/cm^2 attained the maximum ammonia-N concentration measured in this study. Results showed accumulation of nitrites could have played a role in denitrification of HTL-AP pre-storage since in other reports high nitrites intermediaries' presence is related to conversion of nitrite-N to ammonia-N to nitrogen gas (Ghazouani et al., 2015).

In the same way, in the post-storage HTL-AP, when the initial organic matter concentration was low as well as the initial inorganic nitrogen availability and despite no detectable levels of nitrite-N being observed during the treatment, 50 mA/cm^2 seemed to have favored denitrification of the HTL-AP post-storage as well (Table S3 in the Supplementary Material).

By looking at the overall measurements of inorganic nitrogen present in the HTL-AP before and after storage, it is distinguishable that a higher concentration of organic matter enables higher accumulation of inorganic nitrogen forms in the wastewater after electrolysis at all the current densities tested in this study, including 50 mA/cm^2. After the poor performance in nitrification of the 50 mA/cm^2 current density and after treating the pre-storage HTL-AP, approximately 888 mg/L of inorganic nitrogen was detected compared to 16 mg/L of inorganic nitrogen observed in the post-storage HTL-AP.

3.4. Effect of current on organic compounds in HTL-AP

At the three current densities tested in this study, it was possible to mineralize heterocycles into intermediary products and fatty acids. By comparing the peak area of the gas chromatography analysis before and after treatment, the removal and accumulation of compounds in the HTL-AP was measured and is displayed in Fig. 6.

With electrolysis of food waste HTL-AP, production of nitrate-N was achieved as well as removal of heterocyclic nitrogen. Fig. 6 details the removal of compounds such as ketones and heterocyclic amines after electrolysis. It also shows differences in degradation products at the operational conditions tested. For example, the propanoic acid peak area increased after the treatment with electrolysis at 30 mA/cm^2. While the graph displays the removal and accumulation of some compounds, the analysis showed the presence of compounds that emerged as products of the treatment such as 2-piperidine, which is a secondary amine with a larger peak area at 10 mA/cm^2, 2-methyl propanoic acid with a larger peak area at 30 mA/cm^2, and acetonitrile with a larger peak area at 30 mA/cm^2 in HTL-AP after electrolysis (Table S4 of Supplemental Material).

Furthermore, incomplete oxidation of heterocyclic amines in the treatment could have been caused by lack of formation of hydroxyl radicals on the surface of the electrode, as explained in a study of oxidation of pyridine into ammonia-N, nitrate-N, and nitrogen gas

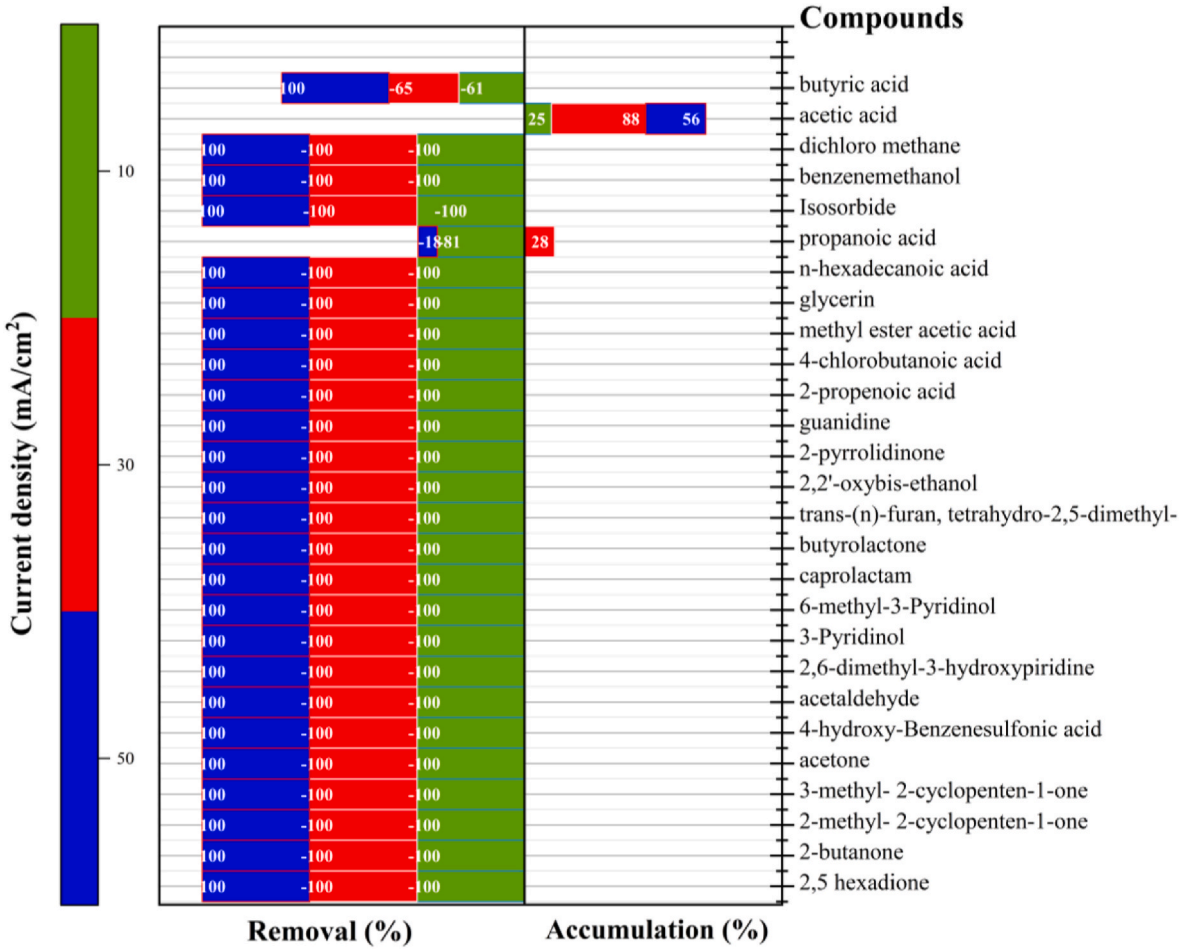

Fig. 6. Gas chromatography analysis after electrolysis of the aqueous phase of hydrothermal liquefaction food mixture, pre-storage, at 10 mA/cm^2, 30 mA/cm^2, and 50 mA/cm^2.

(Jiang et al., 2021a). As observed in studies of the oxidation of organic compounds with anodic oxidation using BDD, complete mineralization is difficult to achieve even at higher current levels without the addition of a supporting electrolyte to enhance oxidation of compounds present in the wastewater (Candia-Onfray et al., 2018).

At the lowest current density, carboxylic acids were completely removed from the HTL-AP. Conversely, carboxylic acids increased in concentration after electrolysis with the higher current densities (30 mA/cm^2 and 50 mA/cm^2). The production of the mentioned compounds could be due to the cleavage of nitrogen in the heterocyclic amines to produce small molecules of carboxylic acids and ammonia-N (Jiang et al., 2021a).

As previous studies have reported, the production of free radicals like hydroxyl radicals could change the structure of the nitrogen cyclic compounds like pyridine to produce smaller molecules such as carboxylic acids and ammonia-N, as well as other carbon compounds products of the mineralization (Jiang et al., 2021b). At higher current densities, there was an increase in carbon reactions since incomplete mineralization of amines or nitrogen compounds was observed. Additionally, there was greater removal of carboxylic acids, or preference for carbon reactions. Among the remaining carbon compounds were acetic acid and propanoic acid.

4. Conclusions

Unlike previous studies that applied advanced oxidation techniques on microalgal derived HTL-AP, this is the first study treating a food derived HTL-AP with a low total nitrogen concentration with electrolysis to recover inorganic nitrogen for its future use as a nutrient solution for plant growth. Electrolysis of raw HTL-AP was completed at ambient environmental conditions, leading to the removal of COD, as well as conversion of nitrogen cyclic compounds into inorganic forms of nitrogen utilizing the BDD anode and SS cathode. The electrodes used in this study performed best for COD removal at 30 mA/cm^2 by removing 61% of the oxidizable organic matter in the HTL-AP. Among the current densities tested, 30 mA/cm^2 and 10 mA/cm^2 showed higher accumulation of nitrate-N in the electrolysis process. A total of 609.4 mg/L and 156.3 mg/L of nitrate-N was accumulated in the HTL-AP, pre-storage, at 10 mA/cm^2 and 30 mA/cm^2, respectively. The highest current density of 50 mA/cm^2 led to a greater removal of COD during the first 4 h of treatment (2 A h) and overall removal of inorganic nitrogen forms in the HTL-AP, both pre- and post-storage. This current density could be ideal for removal of organic matter in the HTL-AP through anodic oxidation. Initial results showed promise to recover nitrate-N from organic nitrogen compounds at lower current densities with electrolysis. This study confirmed that electrolysis can reduce the nutrient imbalance of the HTL-AP, while increasing the overall inorganic nitrogen availability in the wastewater.

Furthermore, results showed increased inorganic nitrogen recovery with higher initial concentrations of organic matter, in addition to changes in the pH and ammonia-N in the HTL-AP after aging and storage. Subsequent studies should focus on the carbon and nitrogen ratio effect on the inorganic nitrogen recovery from the HTL-AP as well as the best storage conditions for HTL-AP to avoid organic compound losses. These findings highlight the significance of storage on nutrient losses before the application of recovery treatments, suggesting that new methods need to be applied to alleviate nutrient losses. Proper storage methods are essential to preserve the water quality characteristics to leverage nutrients efficiently and raise the valorization of the HTL-AP.

Furthermore, this study explored the effects of storage on the recovery of nutrients of a biomass derived byproduct (HTL-AP), which is thermochemically unstable. Previous studies have overlooked the effects of storage on the chemical composition of the HTL-AP and the nutrient recovery. This study has explored the interaction between the initial organic load and the nitrate-N recovery, suggesting that a higher organic concentration leads to higher yields of the desired inorganic nitrogen forms in the HTL-AP.

Funding sources

This work was supported by United States Department of Agriculture (USDA) National Institute of Food and Agriculture's (NIFA) Bioproduct Pilot Program (2023-79000-38974, 2023), a Fulbright scholarship awarded by the U.S. Department of State, and the Department of Agricultural and Biological Engineering, University of Illinois, Urbana-Champaign.

Data availability

No data associated with this study has been deposited into a publicly available repository. Data will be available upon request.

CRediT authorship contribution statement

Barbara Camila Bogarin Cantero: Writing – original draft, Visualization, Methodology, Investigation, Formal analysis, Data curation, Conceptualization. **Yuanhui Zhang:** Writing – review & editing, Supervision, Project administration, Funding acquisition. **Paul C. Davidson:** Writing – review & editing, Supervision, Resources, Project administration, Methodology.

Declaration of competing interest

The authors declare that they have no known competing financial interests or personal relationships that could have appeared to influence the work reported in this paper.

Data availability

Data will be made available on request.

Acknowledgments

The authors would like to acknowledge the support of many student members of the Davidson Research Team and the Environmental and Enhancing Energy (E2E) laboratory from the University of Illinois at Urbana Champaign for providing the materials to complete this study.

Appendix A. Supplementary data

Supplementary data to this article can be found online at https://doi.org/10.1016/j.envpol.2024.125069.

References

Aierzhati, A., Stablein, M.J., Wu, N.E., Kuo, C.T., Si, B., Kang, X., Zhang, Y., 2019. Experimental and model enhancement of food waste hydrothermal liquefaction with combined effects of biochemical composition and reaction conditions. Bioresour. Technol. 284, 139–147. https://doi.org/10.1016/J.BIORTECH.2019.03.076.

Aierzhati, A., Watson, J., Si, B., Stablein, M., Wang, T., Zhang, Y., 2021. Development of a mobile, pilot scale hydrothermal liquefaction reactor: food waste conversion product analysis and techno-economic assessment. Energy Convers. Manag. X 10, 100076. https://doi.org/10.1016/J.ECMX.2021.100076.

Anglada, Á., Urtiaga, A., Ortiz, I., 2009. Contributions of electrochemical oxidation to waste-water treatment: fundamentals and review of applications. J. Appl. Chem. Biotechnol. 84 (12), 1747–1755. https://doi.org/10.1002/JCTB.2214.

Biller, P., Ross, A.B., Skill, S.C., Lea-Langton, A., Balasundaram, B., Hall, C., Riley, R., Llewellyn, C.A., 2012. Nutrient recycling of aqueous phase for microalgae cultivation from the hydrothermal liquefaction process. Algal Res. 1 (1), 70–76. https://doi.org/10.1016/J.ALGAL.2012.02.002.

Cabeza, A., Urtiaga, A., Rivero, M.J., Ortiz, I., 2007. Ammonium removal from landfill leachate by anodic oxidation. J. Hazard Mater. 144 (3), 715–719. https://doi.org/10.1016/J.JHAZMAT.2007.01.106.

Candia-Onfray, C., Espinoza, N., Sabino da Silva, E.B., Toledo-Neira, C., Espinoza, L.C., Santander, R., García, V., Salazar, R., 2018. Treatment of winery wastewater by anodic oxidation using BDD electrode. Chemosphere 206, 709–717. https://doi.org/10.1016/J.CHEMOSPHERE.2018.04.175.

Chen, J., Zhang, J., Pan, W., An, G., Deng, Y., Li, Y., Hu, Y., Xiao, Y., Liu, T., Leng, S., Chen, J., Li, J., Peng, H., Leng, L., Zhou, W., 2022. A novel strategy to simultaneously enhance bio-oil yield and nutrient recovery in sequential hydrothermal liquefaction of high protein microalgae. Energy Convers. Manag. 255, 115330. https://doi.org/10.1016/J.ENCONMAN.2022.115330.

Chen, P.H., Venegas Jimenez, J.L., Rowland, S.M., Quinn, J.C., Laurens, L.M.L., 2020. Nutrient recycle from algae hydrothermal liquefaction aqueous phase through a novel selective remediation approach. Algal Res. 46, 101776. https://doi.org/10.1016/J.ALGAL.2019.101776.

Ciarlini, J., Alves, L., Rajarathnam, G.P., Haynes, B.S., Montoya, A., 2020a. Electrochemical oxidation of nitrogen-rich post-hydrothermal liquefaction wastewater. Algal Res. 48, 101919. https://doi.org/10.1016/J.ALGAL.2020.101919.

Ciarlini, J., Alves, L., Rajarathnam, G.P., Haynes, B.S., Montoya, A., 2020b. Electrochemical oxidation of nitrogen-rich post-hydrothermal liquefaction wastewater. Algal Res. 48, 101919. https://doi.org/10.1016/J.ALGAL.2020.101919.

Ciríaco, L., Anjo, C., Correia, J., Pacheco, M.J., Lopes, A., 2009. Electrochemical degradation of Ibuprofen on Ti/Pt/PbO2 and Si/BDD electrodes. Electrochim. Acta 54 (5), 1464–1472. https://doi.org/10.1016/J.ELECTACTA.2008.09.022.

Díaz, V., Ibáñez, R., Gómez, P., Urtiaga, A.M., Ortiz, I., 2011. Kinetics of electro-oxidation of ammonia-N, nitrites and COD from a recirculating aquaculture saline water system using BDD anodes. Water Res. 45 (1), 125–134. https://doi.org/10.1016/J.WATRES.2010.08.020.

dos Santos, A.J., Fajardo, A.S., Kronka, M.S., Garcia-Segura, S., Lanza, M.R.V., 2021. Effect of electrochemically-driven technologies on the treatment of endocrine disruptors in synthetic and real urban wastewater. Electrochim. Acta 376, 138034. https://doi.org/10.1016/J.ELECTACTA.2021.138034.

Egerland Bueno, B., Américo Soares, L., Quispe-Arpasi, D., Kimiko Sakamoto, I., Zhang, Y., Amancio Varesche, M.B., Ribeiro, R., Tommaso, G., 2020. Anaerobic digestion of aqueous phase from hydrothermal liquefaction of Spirulina using biostimulated sludge. Bioresour. Technol. 312, 123552. https://doi.org/10.1016/J.BIORTECH.2020.123552.

Fil, B.A., Boncukcuoglu, R., Yilmaz, A.E., Bayar, S., 2014. Electro-oxidation of pistachio processing industry wastewater using graphite anode. CLEAN – Soil, Air, Water 42 (9), 1232–1238. https://doi.org/10.1002/CLEN.201300560.

Forster, R.J., 2019. Voltammetry | cyclic voltammetry of organic compounds. Encyclopedia of Analytical Science 197–208. https://doi.org/10.1016/B978-0-12-409547-2.14488-9.

Garcia Alba, L., Torri, C., Fabbri, D., Kersten, S.R.A., Wim Brilman, D.W.F., 2013. Microalgae growth on the aqueous phase from Hydrothermal Liquefaction of the same microalgae. Chem. Eng. J. 228, 214–223. https://doi.org/10.1016/J.CEJ.2013.04.097.

Ghazouani, M., Akrout, H., Bousselmi, L., 2015. Efficiency of electrochemical denitrification using electrolysis cell containing BDD electrode. Desalination Water Treat. 53 (4), 1107–1117. https://doi.org/10.1080/19443994.2014.884473.

Ghazouani, M., Akrout, H., Bousselmi, L., 2017. Nitrate and carbon matter removals from real effluents using Si/BDD electrode. Environ. Sci. Pollut. Control Ser. 24 (11), 9895–9906. https://doi.org/10.1007/S11356-016-7563-7/FIGURES/9.

Godwin, C.M., Hietala, D.C., Lashaway, A.R., Narwani, A., Savage, P.E., Cardinale, B.J., 2017. Algal polycultures enhance coproduct recycling from hydrothermal liquefaction. Bioresour. Technol. 224, 630–638. https://doi.org/10.1016/J.BIORTECH.2016.11.105.

Halleraker, H.v., Barth, T., 2020. Quantitative NMR analysis of the aqueous phase from hydrothermal liquefaction of lignin. J. Anal. Appl. Pyrol. 151, 104919. https://doi.org/10.1016/J.JAAP.2020.104919.

Harisankar, S., Francis Prashanth, P., Nallasivam, J., Vishnu Mohan, R., Vinu, R., 2021. Effects of aqueous phase recirculation on product yields and quality from hydrothermal liquefaction of rice straw. Bioresour. Technol. 342, 125951. https://doi.org/10.1016/J.BIORTECH.2021.125951.

He, S., Zhao, M., Wang, J., Cheng, Z., Yan, B., Chen, G., 2020. Hydrothermal liquefaction of low-lipid algae Nannochloropsis sp. and Sargassum sp.: effect of feedstock composition and temperature. Sci. Total Environ. 712, 135677. https://doi.org/10.1016/J.SCITOTENV.2019.135677.

Hmani, E., Chaabane Elaoud, S., Samet, Y., Abdelhédi, R., 2009. Electrochemical degradation of waters containing O-Toluidine on PbO2 and BDD anodes. J. Hazard Mater. 170 (2–3), 928–933. https://doi.org/10.1016/J.JHAZMAT.2009.05.058.

Hmani, E., Samet, Y., Abdelhédi, R., 2012. Electrochemical degradation of auramine-O dye at boron-doped diamond and lead dioxide electrodes. Diam. Relat. Mater. 30, 1–8. https://doi.org/10.1016/J.DIAMOND.2012.08.003.

Hu, Z., Grasso, D., 2005. WATER ANALYSIS | chemical oxygen demand. In: Encyclopedia of Analytical Science, second ed., pp. 325–330. https://doi.org/10.1016/B0-12-369397-7/00663-4.

Hughes, K., Han, W., Yargeau, V., Omanovic, S., 2023. Electrochemical oxidation of the increasingly used disinfectant benzalkonium chloride. Can. J. Chem. Eng. 101 (6), 3304–3308. https://doi.org/10.1002/CJCE.24842.

Jara, C.C., Martínez-Huitle, C.A., Torres-Palma, R.A., 2009. PORTUGALIAE ELECTROCHIMICA ACTA distribution of nitrogen ions generated in the electrochemical oxidation of nitrogen containing organic compounds. Port. Electrochim. Acta 27 (3), 203–213. https://doi.org/10.4152/pea.200903203.

Jesse, S.D., Davidson, P.C., 2019. Treatment of post-hydrothermal liquefaction wastewater (PHWW) for heavy metals, nutrients, and indicator pathogens. Water 11 (4), 854. https://doi.org/10.3390/W11040854, 2019, Vol. 11, Page 854.

Jesse, S.D., Zhang, Y., Margenot, A.J., Davidson, P.C., 2019. Hydroponic lettuce production using treated post-hydrothermal liquefaction wastewater (PHW). Sustainability 11 (13), 3605. https://doi.org/10.3390/SU11133605, 2019, Vol. 11, Page 3605.

Jiang, H., Fan, L., Cai, C., Hu, Y., Zhao, F., Ruan, R., Yang, W., 2020. Study on the bio-oil characterization and heavy metals distribution during the aqueous phase recycling in the hydrothermal liquefaction of As-enriched Pteris vittata L. Bioresour. Technol. 317, 124031. https://doi.org/10.1016/J.BIORTECH.2020.124031.

Jiang, H., Zhang, R., Hao, J., Xu, X., Chen, J., Zhang, Y., Yang, F., 2021a. Design, preparation, characterization, and application of MnxCu1-xOy/γ-Al2O3 catalysts in ozonation to achieve simultaneous organic carbon and nitrogen removal in pyridine wastewater. Sci. Total Environ. 774, 145189. https://doi.org/10.1016/J.SCITOTENV.2021.145189.

Jiang, H., Zhang, R., Hao, J., Xu, X., Chen, J., Zhang, Y., Yang, F., 2021b. Design, preparation, characterization, and application of MnxCu1-xOy/γ-Al2O3 catalysts in ozonation to achieve simultaneous organic carbon and nitrogen removal in pyridine wastewater. Sci. Total Environ. 774, 145189. https://doi.org/10.1016/J.SCITOTENV.2021.145189.

Kohansal, K., Toor, S., Sharma, K., Chand, R., Rosendahl, L., Pedersen, T.H., 2021. Hydrothermal liquefaction of pre-treated municipal solid waste (biopulp) with recirculation of concentrated aqueous phase. Biomass Bioenergy 148, 106032. https://doi.org/10.1016/J.BIOMBIOE.2021.106032.

Leme, V.F.C., Lopez, K., Costa, T., Conerty, B., Leonelli, L.B., Zhang, Y., Davidson, P.C., 2024a. Hydrothermal liquefaction aqueous phase mycoremediation to increase inorganic nitrogen availability. Heliyon 10 (11), e31992. https://doi.org/10.1016/j.heliyon.2024.e31992.

Leme, V.F.C., Lopez, K., Costa, T., Conerty, B., Leonelli, L.B., Zhang, Y., Davidson, P.C., 2024b. Hydrothermal liquefaction aqueous phase mycoremediation to increase inorganic nitrogen availability. Heliyon 10 (11), e31992. https://doi.org/10.1016/j.heliyon.2024.e31992.

Leng, L., Li, J., Wen, Z., Zhou, W., 2018. Use of microalgae to recycle nutrients in aqueous phase derived from hydrothermal liquefaction process. Bioresour. Technol. 256, 529–542. https://doi.org/10.1016/J.BIORTECH.2018.01.121.

Leng, L., Zhang, W., Leng, S., Chen, J., Yang, L., Li, H., Jiang, S., Huang, H., 2020. Bioenergy recovery from wastewater produced by hydrothermal processing biomass: progress, challenges, and opportunities. Sci. Total Environ. 748, 142383. https://doi.org/10.1016/J.SCITOTENV.2020.142383.

León, M., Marcilla, A.F., García, Á.N., 2019. Hydrothermal liquefaction (HTL) of animal by-products: influence of operating conditions. Waste Manag. 99, 49–59. https://doi.org/10.1016/J.WASMAN.2019.08.022.

Liu, G., Du, H., Sailikebuli, X., Meng, Y., Liu, Y., Wang, H., Zhang, J., Wang, B., Saad, M. G., Li, J., Wang, W., 2021. Evaluation of storage stability for biocrude derived from hydrothermal liquefaction of microalgae. Energy Fuel. 35 (13), 10623–10629. https://doi.org/10.1021/ACS.ENERGYFUELS.1C01386/ASSET/IMAGES/LARGE/EF1C01386_0002.JPEG.

Lopez, K., Leme, V.F.C., Warzecha, M., Davidson, P.C., 2024. Wastewater nutrient recovery via fungal and nitrifying bacteria treatment. Agriculture 14 (4), 580. https://doi.org/10.3390/AGRICULTURE14040580, 2024, Vol. 14, Page 580.

Maddi, B., Panisko, E., Wietsma, T., Lemmon, T., Swita, M., Albrecht, K., Howe, D., 2017. Quantitative characterization of aqueous byproducts from hydrothermal liquefaction of municipal wastes, food industry wastes, and biomass grown on waste. ACS Sustain. Chem. Eng. 5 (3), 2205–2214. https://doi.org/10.1021/ACSSUSCHEMENG.6B02367/ASSET/IMAGES/LARGE/SC-2016-02367R_0007.JPEG.

McGinn, P.J., Park, K.C., Robertson, G., Scoles, L., Ma, W., Singh, D., 2019. Strategies for recovery and recycling of nutrients from municipal sewage treatment effluent and hydrothermal liquefaction wastewaters for the growth of the microalga Scenedesmus sp. AMDD. Algal Res. 38, 101418. https://doi.org/10.1016/J.ALGAL.2019.101418.

Olvera-Vargas, H., Oturan, N., Brillas, E., Buisson, D., Esposito, G., Oturan, M.A., 2014. Electrochemical advanced oxidation for cold incineration of the pharmaceutical ranitidine: mineralization pathway and toxicity evolution. Chemosphere 117 (1), 644–651. https://doi.org/10.1016/J.CHEMOSPHERE.2014.09.084.

Panizza, M., Michaud, P.A., Cerisola, G., Comninellis, C.H., 2001a. Anodic oxidation of 2-naphthol at boron-doped diamond electrodes. J. Electroanal. Chem. 507 (1–2), 206–214. https://doi.org/10.1016/S0022-0728(01)00398-9.

Panizza, M., Michaud, P.A., Cerisola, G., Comninellis, C.H., 2001b. Anodic oxidation of 2-naphthol at boron-doped diamond electrodes. J. Electroanal. Chem. 507 (1–2), 206–214. https://doi.org/10.1016/S0022-0728(01)00398-9.

Pedersen, T.H., Grigoras, I.F., Hoffmann, J., Toor, S.S., Daraban, I.M., Jensen, C.U., Iversen, S.B., Madsen, R.B., Glasius, M., Arturi, K.R., Nielsen, R.P., Søgaard, E.G., Rosendahl, L.A., 2016. Continuous hydrothermal co-liquefaction of aspen wood and glycerol with water phase recirculation. Appl. Energy 162, 1034–1041. https://doi.org/10.1016/J.APENERGY.2015.10.165.

Ren, S., Ye, X.P., 2018. Stability of crude bio-oil and its water-extracted fractions. J. Anal. Appl. Pyrol. 132, 151–162. https://doi.org/10.1016/J.JAAP.2018.03.005.

Reynolds, L.P., Leme, V.F.C., Davidson, P.C., 2024. Investigating the impacts of wastewaters on lettuce (Lactuca sativa) seed germination and growth. Agriculture 14 (4), 608. https://doi.org/10.3390/AGRICULTURE14040608, 2024, Vol. 14, Page 608.

Rodrigo, M.A., Michaud, P.A., Duo, I., Panizza, M., Cerisola, G., Comninellis, Ch, 2001. Oxidation of 4-chlorophenol at boron-doped diamond electrode for wastewater treatment. J. Electrochem. Soc. 148 (5), D60. https://doi.org/10.1149/1.1362545/XML.

Savvas, D., Passam, H.C., Olympios, C., Nasi, E., Moustaka, E., Mantzos, N., Barouchas, P., 2006. Effects of ammonium nitrogen on lettuce grown on pumice in a closed hydroponic system. Hortscience 41 (7), 1667–1673. https://doi.org/10.21273/HORTSCI.41.7.1667.

Si, B., Yang, L., Zhou, X., Watson, J., Tommaso, G., Chen, W.T., Liao, Q., Duan, N., Liu, Z., Zhang, Y., 2019. Anaerobic conversion of the hydrothermal liquefaction aqueous phase: fate of organics and intensification with granule activated carbon/ozone pretreatment. Green Chem. 21 (6), 1305–1318. https://doi.org/10.1039/C8GC02907E.

Summers, S., Valentine, A., Wang, Z., Zhang, Y., 2023. Pilot-Scale continuous plug-flow hydrothermal liquefaction of food waste for biocrude production. Ind. Eng. Chem. Res. 62 (31), 12174–12182. https://doi.org/10.1021/ACS.IECR.3C01587/ASSET/IMAGES/LARGE/IE3C01587_0007.JPEG.

SundarRajan, P., Gopinath, K.P., Arun, J., GracePavithra, K., Adithya Joseph, A., Manasa, S., 2021a. Insights into valuing the aqueous phase derived from hydrothermal liquefaction. Renew. Sustain. Energy Rev. 144, 111019. https://doi.org/10.1016/J.RSER.2021.111019.

SundarRajan, P., Gopinath, K.P., Arun, J., GracePavithra, K., Adithya Joseph, A., Manasa, S., 2021b. Insights into valuing the aqueous phase derived from hydrothermal liquefaction. Renew. Sustain. Energy Rev. 144, 111019. https://doi.org/10.1016/J.RSER.2021.111019.

Sundén, B., 2019. Electrochemistry and thermodynamics. Hydrogen, Batteries and Fuel Cells 15–36. https://doi.org/10.1016/B978-0-12-816950-6.00002-6.

Swetha, A., ShriVigneshwar, S., Gopinath, K.P., Sivaramakrishnan, R., Shanmuganathan, R., Arun, J., 2021a. Review on hydrothermal liquefaction aqueous phase as a valuable resource for biofuels, bio-hydrogen and valuable bio-chemicals recovery. Chemosphere 283, 131248. https://doi.org/10.1016/J.CHEMOSPHERE.2021.131248.

Swetha, A., ShriVigneshwar, S., Gopinath, K.P., Sivaramakrishnan, R., Shanmuganathan, R., Arun, J., 2021b. Review on hydrothermal liquefaction aqueous phase as a valuable resource for biofuels, bio-hydrogen and valuable bio-chemicals recovery. Chemosphere 283, 131248. https://doi.org/10.1016/J.CHEMOSPHERE.2021.131248.

Tenne, R., Patel, K., Hashimoto, K., Fujishima, A., 1993. Efficient electrochemical reduction of nitrate to ammonia using conductive diamond film electrodes. J. Electroanal. Chem. 347 (1–2), 409–415. https://doi.org/10.1016/0022-0728(93)80105-Q.

Wang, H., Xu, J., Liu, X., Sheng, L., 2021. Preparation of straw activated carbon and its application in wastewater treatment: a review. J. Clean. Prod. 283, 124671. https://doi.org/10.1016/J.JCLEPRO.2020.124671.

Wang, Z., Watson, J., Wang, T., Yi, S., Si, B., Zhang, Y., 2021. Enhancing energy recovery via two stage co-fermentation of hydrothermal liquefaction aqueous phase and crude glycerol. Energy Convers. Manag. 231, 113855. https://doi.org/10.1016/J.ENCONMAN.2021.113855.

Watson, J., Wang, T., Si, B., Chen, W.T., Aierzhati, A., Zhang, Y., 2020. Valorization of hydrothermal liquefaction aqueous phase: pathways towards commercial viability. Prog. Energy Combust. Sci. 77, 100819. https://doi.org/10.1016/J.PECS.2019.100819.

Wu, B., Berg, S.M., Remucal, C.K., Strathmann, T.J., 2020. Evolution of N-containing compounds during hydrothermal liquefaction of sewage sludge. ACS Sustain. Chem. Eng. 8 (49), 18303–18313. https://doi.org/10.1021/ACSSUSCHEMENG.0C07060/ASSET/IMAGES/LARGE/SC0C07060_0007.JPEG.

Yang, L., Si, B., Zhang, Y., Watson, J., Stablein, M., Chen, J., Zhang, Y., Zhou, X., Chu, H., 2020. Continuous treatment of hydrothermal liquefaction wastewater in an anaerobic biofilm reactor: potential role of granular activated carbon. J. Clean. Prod. 276, 122836. https://doi.org/10.1016/J.JCLEPRO.2020.122836.

Zhao, H., Jiang, D., Zhang, S., Catterall, K., John, R., 2004. Development of a direct photoelectrochemical method for determination of chemical oxygen demand. Anal. Chem. 76 (1), 155–160. https://doi.org/10.1021/AC0302298/ASSET/IMAGES/LARGE/AC0302298F00005.JPEG.

Zhu, Y., Jones, S.B., Schmidt, A.J., Albrecht, K.O., Edmundson, S.J., Anderson, D.B., 2019. Techno-economic analysis of alternative aqueous phase treatment methods for microalgae hydrothermal liquefaction and biocrude upgrading system. Algal Res. 39, 101467. https://doi.org/10.1016/J.ALGAL.2019.101467.

Zhu, Z., Rosendahl, L., Toor, S.S., Yu, D., Chen, G., 2015. Hydrothermal liquefaction of barley straw to bio-crude oil: effects of reaction temperature and aqueous phase recirculation. Appl. Energy 137, 183–192. https://doi.org/10.1016/J.APENERGY.2014.10.005.

Zöllig, H., Remmele, A., Morgenroth, E., Udert, K.M., 2017. Removal rates and energy demand of the electrochemical oxidation of ammonia and organic substances in real stored urine. Environmental Science: Water Research & Technology 3 (3), 480–491. https://doi.org/10.1039/C7EW00014F.